Nuclear Materials Authority
P.O.Box 530 Maadi, Cairo, Egypt

DOAJ DIRECTORY OF OPEN ACCESS JOURNALS

ISSN 2314-5609
Nuclear Sciences Scientific Journal
9A, 21- 32
2020
http://www.ssnma.com

# IMPACT OF STRUCTURAL ELEMENTS ON THE SPATIAL DISTRIBUTION OF THE MINERALIZED ZONES IN WADI ATALLA ENVIRON, CENTRAL EASTERN DESERT, EGYPT

HARIDY M. M. HARIDY
*Nuclear Materials Authority, Cairo, Egypt*

## ABSTRACT

Wadi Atalla area is located between Lat. 25° 59' to 26° 23' N and Long. 33° 10' to 33° 40' E (Fig. 1). It includes some of the most promising uranium occurrences which are related to the younger granitic plutons such as Um Had, Kab Amiri and El Erediya as well as several old gold mines such as El Erediya, Atalla, El Fawakhir, El Sid and Hamama. In addition to numerous ancient gold excavations along a huge NW-SE shear zone extends about 80 km from El Erediya in the north to El Fawakhir in the south.

Field measurement supported with analysis of the structural lineaments of the Landsat image also the geological map shows that most of the well-developed structural lineaments have NW-SE, NE-SW and N-S trends. The fault patterns as delineated from Landsat image are well matched with that obtained from the correlogram driving from gravity and topographic data.

Mineralization found along NW-SE fault zones appear as linear patterns. The mineralization of uranium and gold are controlled in their spatial distribution by fault tectonics and basic magmatic rocks occurring along these NW-SE sub-parallel faults.

A set of radioelements (eU ppm, eTh ppm and K%) contour maps were prepared. They are superimposed individually on the geological map to delineate uranium potentiality. The constructed maps revealed that the southern parts of both Kab Amiri and Um Had plutons as well as the northwestern part of El Erediya pluton are promising zones for uranium potentiality.

## INTRODUCTION

Wadi Atalla running in the direction NW-SE connecting between Qena-Safaga and Qift-Al Quseir paved roads that traverse the region approximately ENE-WSW. Along it many uranium and gold prospect areas were found including El Misskat and El Erediya uranium prospect and Atalla, Serbax, Abu Marawat, Hamama and Fawakir-El Sid gold deposits. The region is underlain by the basement complex of Precambrian rocks that are part of the Nubian Shield.

The main purpose of this work is to integrate the available airborne spectrometric and gravity data as well as satellite remote sensing data with the field structural investigations in order to explain the structural factors controlling mineralization in this area. These goals are achieved by manipulating various data sets separately and then integrating them together.

The autocorrelogram function is applied

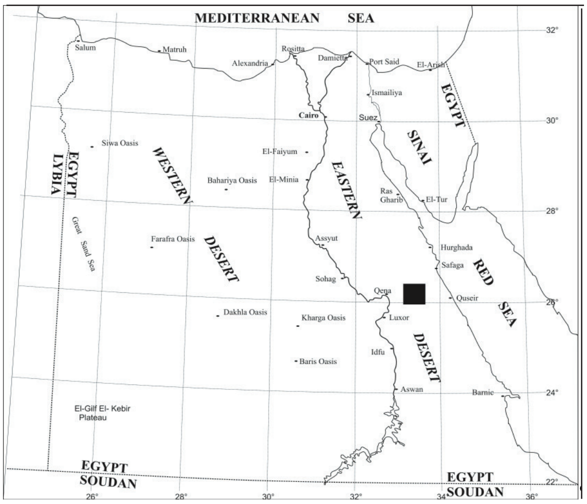


■ The study area

Fig. 1 : location map of the study area

on the topographic and gravity data, while the statistical trend analysis is carried out on the traced structural lineaments to reveal the structural trends affecting the area.

## GEOLOGICAL SETTING

The regional geology of the area (Fig. 2) is included in the Conoco Coral (1986) geologic map with scale 1:500,000. It comprises (from the oldest) ophiolitic serpentinite, metagabbro, metavolcanics, metasediments, Hammamat clastics, younger granites, post Hammamat felsite, Galala Formation and Taref Formation. The Precambrian rocks are dissected by numerous post granitic dykes of various compositions and traversed by several Wadis filled with Quaternary alluvium deposits.

The Eastern Desert has been subdivided into three tectono-stratigraphic domains; North Eastern Desert (NED), Central Eastern Desert (CED) and South Eastern Desert (SED), (Stern and Hedge, 1985). The CED is dominated by a strong NW-SE structural trend expressed in steeply dipping ductile-brittle shear zones and dissected by ENE deep-seated faults (Greiling et al., 1988).

Garson and Krs (1976) proposed a series of crustal blocks in the Eastern Desert formed by faulting along N60°E trend, the age of block faulting is uncertain, but it was probably initiated in the Precambrian. They also identified large scale shear zones and deep-seated tectonic fractures, generally, trending N30°W and N60°E which they believed to be related to the rifting and opening of the Red Sea. Such features are thought to have controlled the geographic distribution of the intrusions in the Red Sea region.

## MINERALIZATION

It was noted that there is a certain linear pattern in the spatial distribution of localities of the well known gold and uranium deposits in the study area (Fig. 3). The linear arrangement of the uranium and gold deposits starts from Fatira, Abu Marawat, Hamama, Gidami, Semna, Abu Grahish, Seg, Kab Amiri, El Erediya, Atalla El Murr, Atalla, Rabshi, Um Esh, Um Had, El Fawakhir and El Sid in the south and extends outside the study area through El Baramiya forming a uranium-gold belt trending NW-SE.

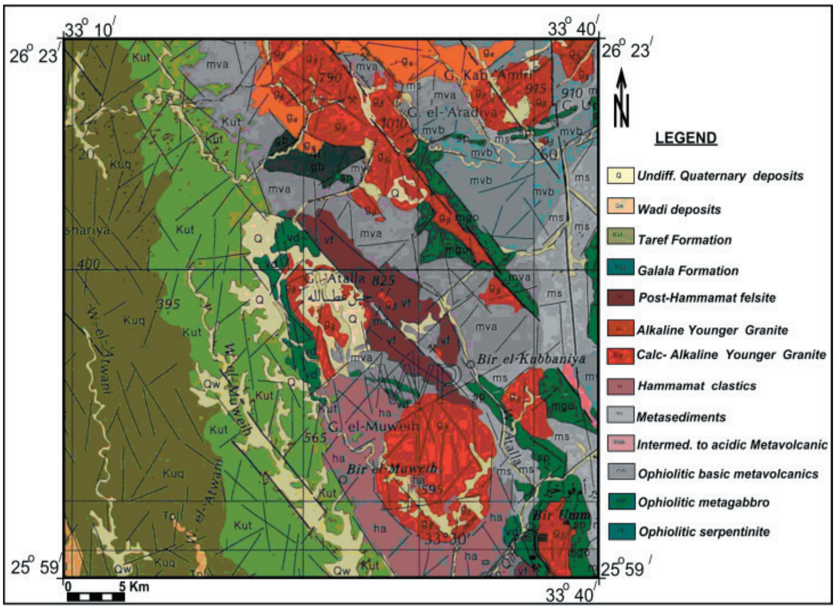


Fig. 2: Geological map of Wadi Atalla area, Central Eastern Desert, Egypt (Conoco Coral, 1986)

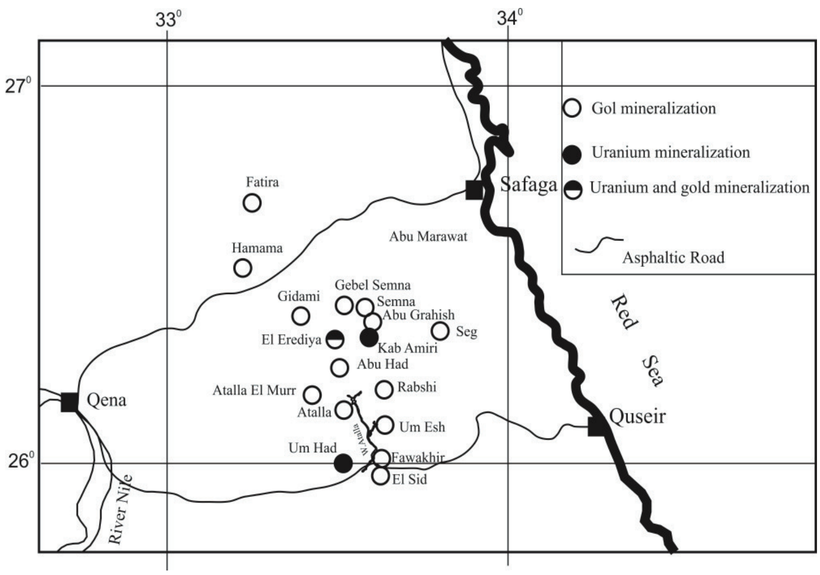


Fig. 3: Location map of gold and uranium mineralization in the study area (The Mineral Map of Egypt, 1994)

Uranium-Th deposits are reported as structurally controlled mineralization in El Erediya (El Kassas, 1974) and Kab Amiri areas (Bakhit, 1975 and Abdel Meguid et. al., 2004). The best examples in the study area for gold vein deposits occurrences are Abu Grahish, Kab Amiri, El Erediya, Abu Had, Rabshi, Atalla El Murr, Atalla, Um Esh, Um Had, Hammamat, El Fawakhir and El Sid areas. They are structurally controlled by the NE-SW and NW-SE trends (Mussa and Abu El Leil, 1983) occurring as vein type mineralization, being fissure fillings, confined to fault planes, or zones of intensive fracturing.

The area of Wadi Atalla has been targeted for active mineralogical and mining investigations by several workers since the beginning of this century. This is because it includes several gold-bearing quartz veins traversing the different rock units in the area and its surroundings, which have been worked out not only by the Ancient Egyptians but also during consecutive ages. These deposits and ore occurrences; El Sid, Atalla, El Erediya, Semna, Atalla El Murr, Um Esh El Zarga, Fatira and Abu Marawat are structurally controlled, (Table 1). The study area is cross-cutted by various dykes with different strikes from NW-SW to NNW-SSE then N-S and NE-SW.

**Gravity Data Regional Trends**

The gravity regional trends are determined by applying the autocorrelogram function on the GRACE (Gravity Recovery and Climate Experiment) data. GRACE is a joint project by the USA, NASA, German DLR and European ESA agencies. It measures the gravity field of the earth by two satellites approximately 220 kilometers (137 miles) apart on the same path with one ahead of the other. The gravitational field of the earth, which holds the satellites in orbits, will pull the satellites differentially as their orbits change in response to variations in gravity over different regions of the earth.

The constructed gravity contour map (Fig. 4) indicated that the gravity regional trends in the area are the NW-SE, N-S and NE-SW trends reflecting deep seated fracture trends.

Autocorrelogram is a function of two variable lags, (i.e. the distances to the X-and Y-coordinates). It describes the change in the degree of connection between adjacent values of the Z-coordinate as a function of the spatial distance (lag) occurred between adjacent values. Version of this figure, the normalized variance in Z, is the autocorrelation function. Autocovariance function in a way is similar to variogram in kriging. The difference is that, the variogram is based on the raw source data, while the autocovariance function, based on a regular grid, is calculated. Another difference is that the autocovariance function reflects the degree of interdependence between adjacent values of the Z-coordinate while the variogram is the degree of spread in the Z-coordinate. Correlogram assesses spatial patterns and spatial correlation of a grid and indicate how well grid values correlate across the grid. They indicate the underlying trends in the grid and give a measure of the anisotropy of the grid (Schwartz, 1974, Tuma, 1979, Ripley, 1981, Press et. al., 1992, Mitasova and Jaroslav, 1993 and Akai, 1994).

The application of the autocorrelogram function on the gravity data of the study area (Fig. 5) enabled deducing the corresponding major structural trends. This indicated that the major trends affecting the area are the NW-SE, N-S, NE-SW and E-W trends.

**Topographic Data Regional Trends**

The topography regional trends are determined by applying the autocorrelogram function on the SRTM data. SRTM is a digital elevation data for Africa acquired and released by the Shuttle Radar Topography Mission (SRTM) aboard the Space Shuttle Endeavour, launched on February 11$^{th}$, 2000 by the National Aeronautics and Space Administration (NASA). This release includes data for all of the continent, plus the island of Madagascar and the Arabian Peninsula. SRTM flew

Table 1: Summery of different gold and uranium mineralized localities at Wadi Atalla environ

| Area | Host rock of gold and uranium mineralization | Mineralized trends | References |
|---|---|---|---|
| Atalla | En-echelon gold-bearing quartz veins in muscovite granite | NE-SW normal to the shear | Wassef et al., (1973) |
| Atalla El Murr | Gold-bearing quartz veins in rhyolite flows and tuffs | NNW-SSE to NW-SE Parallel to shear zone | |
| Um Esh El Zarga | Bands of fluorite chalcedony and calcite | N - S | El Sokkary and El Kassas, (1976) |
| Sid-Fawakhir | Gold-bearing quartz veins | ENE-WSW and NNE-SSW | Harraz and Ashmawy (1994) |
| Abu Marwat | Hydrothermally altered acidic volcanics | N-S and NW-SW | Botros(1991) |
| | Gold bearing quartz veins | NW-SE | |
| El Sid | Uraniferous quartz veins | E-W | Harraz (1995) |
| | Gold in sheared ophiolite sequences | N-S to NNW-SSE | |
| Hamama | Gold-bearing hematite-rich quartz vein | N-S | Abd El Nabi et al., (1977) |
| Semna | Gold-bearing quartz veins confined to hydrothermal altered shear zone | NNW-SSE | Zoheir et al., (2008c) |
| | Gold-bearing quartz-carbonate veins and lenses | WNW-ESE to NW-SE | |
| Fatira | Gold-bearing silicified pyritized felsite-porphyry dykes | N-W | Klemm and Klemm (2013) |
| El Erediya | Gold-bearing quartz vein hosted by grey granodiorite | NNW-SSE | Mostafa (2013) |
| | U-mineralization along silica vein along shear zone | NW-SE to NNE-SSW and ENE-WSW | |
| Kab Amiri | Vein type mineralization in younger granite | NE-SW and NW-SE fractures | Mussa and Abu El Leil (1983) |
| Um Had | SW rim of the weathered granite | NW-SE | Kamal El-Din, (1986) |

on board the Space Shuttle Endeavour in February, 2000 and used an interferometric radar system to map the topography of Earth's landmass between latitudes 56 degrees south and 60 degrees north.

The constructed topographic contour map (Fig. 6) indicated that the major trends in the area are the NW-SE, N-S, NE-SW and E-W trends.

The application of the autocorrelogram function on the topographic data of the study area (Fig. 7) enabled deducing the corresponding major structural trends. This indicated that the major trends affecting the area are the NW-SE, N-S, NE-SW and E-W trends.

## STRUCTURAL LINEAMENTS ANALYSES

Visual analysis of Landsat image (Fig. 8) was utilized for the identification of lineaments and lithological features associated with uranium mineralization. The lin-

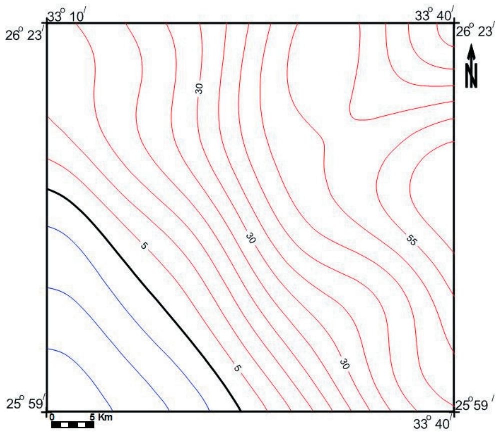


Fig. 4: The contour map of GRACE Gravity Data (in m. gal) of Wadi Atalla area, Central Eastern Desert, Egypt

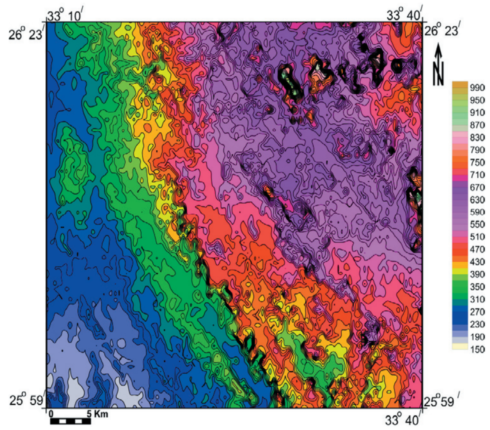


Fig. 6: Contour map of SRTM topographic data of Wadi Atalla area, Central Eastern Desert, Egypt

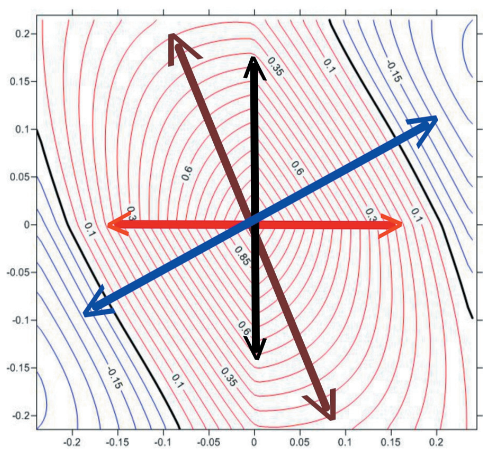


Fig. 5: The correllogram of GRACE gravity data of Wadi Atalla area, Central Eastern Desert, Egypt

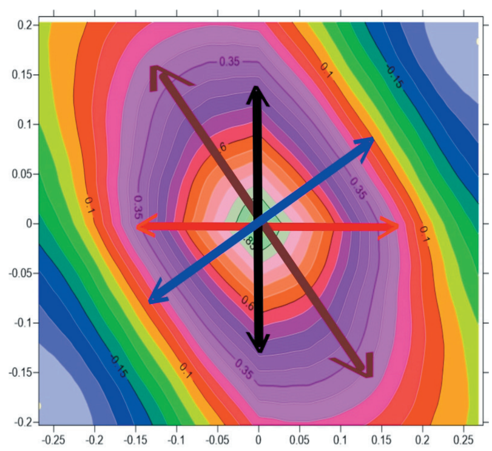


Fig. 7: Autocorrellogram of SRTM topographic Data of Wadi Atalla area, Central Eastern Desert, Egypt

eament (a line feature or pattern interpreted on a remote sensing image) reflects the geological structure such as faults. In this sense, the lineament extraction is very important for the application of remote sensing to geology. Computer generated lineaments would involve all linear features of natural terrain as well as artificial structures (pipe lines, asphaltic roads …etc.) which have to be removed by the interpreter.

So, it should be discriminated from other linear features that are not due to geological structures. Therefore the lineament extraction should be carefully interpreted by geologists. Perfect analysis of lineament information can even allow analysis of the geologi-

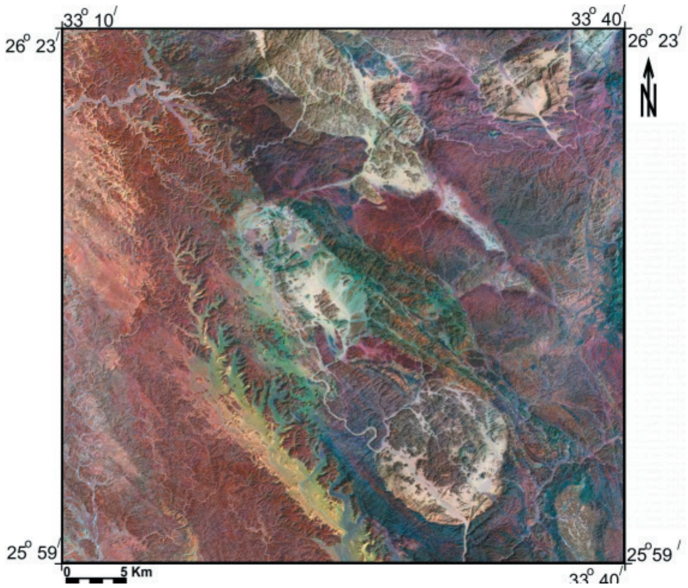


Fig. 8: False color composite Landsat image, Wadi Atalla area, Central Eastern Desert, Egypt (Space Atlas of Misr, 1990)

cal structures and history. Study of Landsat image revealed that the area is formed of different igneous and metamorphic rocks that have been subjected to successive movements since their formation that created different structural features manifested by fractures.

El-Etr (1976) subdivided and classified the structural lineaments by length into megalineaments (>100 Km), macrolineaments (100-10 Km) and *brachylineaments* (10 to 2 Km). The statistical analysis of the extracted structural lineaments allowed constructing the rose diagrams presented on Fig. (9). Most of the well-developed lineaments (in length wise or number wise) have NW-SE, NE-SW and N-S trends. NW-SE lineaments trend is common in all rock exposures in the study area and forming very long wadis and lithological contacts between basement and sedimentary rocks. The structural lineaments maps of the *brachylineaments* (Fig. 9) and *macrolineaments* (Fig. 10) are compiled from Landsat images (1:250,000) and the published geological maps.

The statistical trend analyses of the *brachylineaments* (Fig. 9) shows that the most abundant trends are the NE-SW, NW-SE and N-S respectively according to the numbers, while the trend analysis by length indicates that the most abundant trends are the NW-SE, NE-SW and N-S respectively. The statistical trend analysis of the *macrolineaments* (Fig. 10) exhibits that the most abundant trends are the NW-SE, N-S, NE-SW and NNW-SSE respectively according to the numbers.

The trend analysis of the *macrolineaments* by length indicates the same distribution as number except for the NNW-SSE and NE-SW, where the most abundant trends are the NW-SE, N-S, NNW-SSE and NE-SW respectively.

## SPECTROMETRIC ASPECTS

The eU, eTh and K anomalies maps (Figs. 11, 12 and 13 respectively) are prepared from airborne gamma ray spectrometric survey (Aeroservice, 1984) of the study area. They

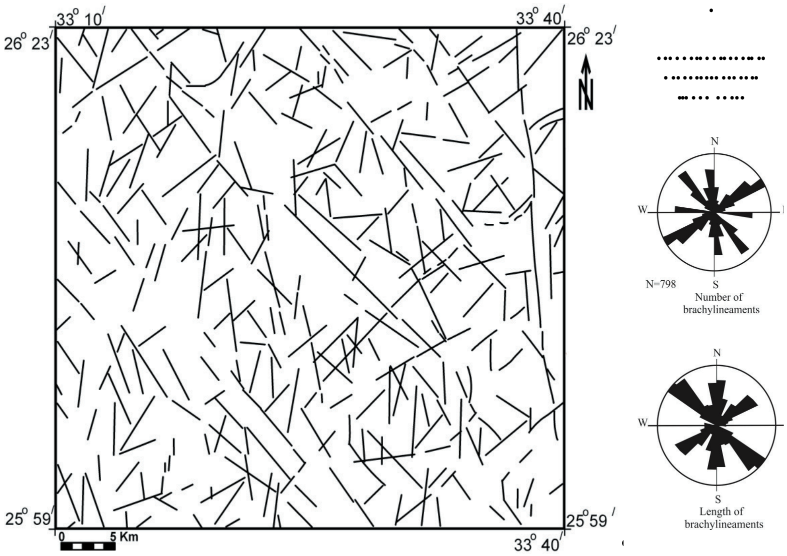


Fig. 9: Brachylineaments map and rose diagrams of the trend distributions by number and length

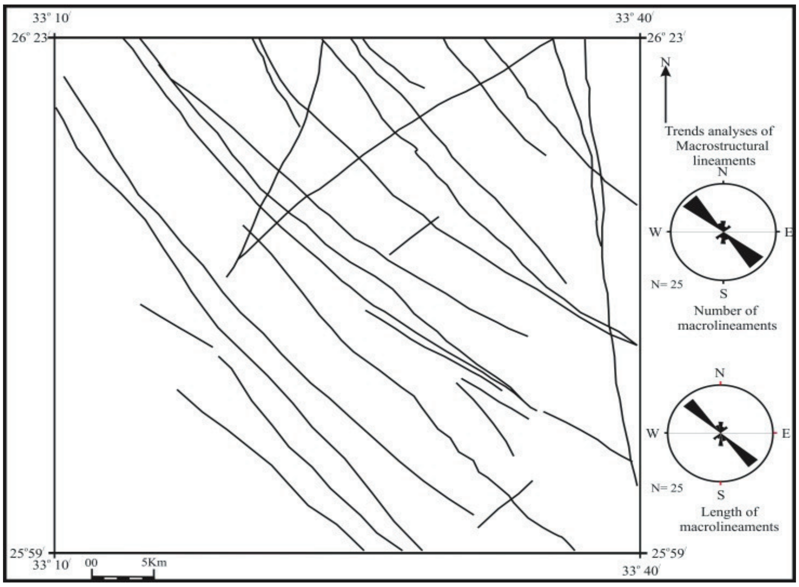


Fig. 10: Macrolineaments map and rose diagrams of the trend distributions by number and length

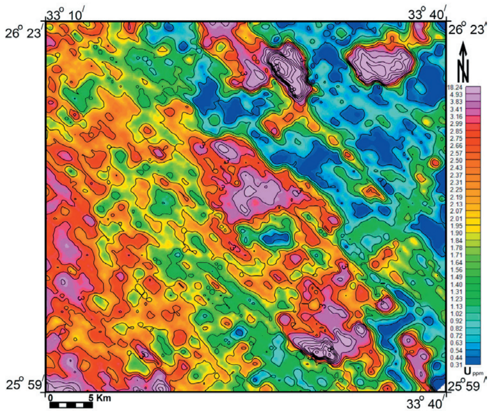


Fig. 11: The eU (ppm) contour map of Wadi Atalla area, Central Eastern Desert, Egypt

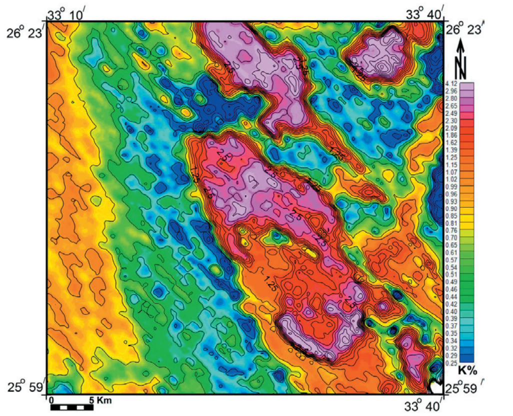


Fig. 13: The K (%) contour map of Wadi Atalla area, Central Eastern Desert, Egypt

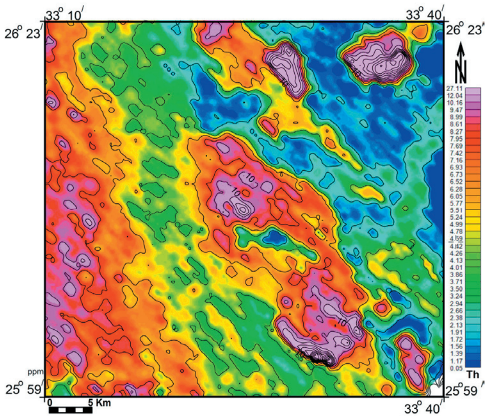


Fig. 12: The eTh (ppm) contour map of Wadi Atalla area, Central Eastern Desert, Egypt

are superimposed individually on the geological map to delineate uranium potentiality. Frequently, it could define clearly the rock boundaries and contacts.

The constructed maps revealed that the radioactive anomalies are distributed mainly in southern parts of both Kab Amiri and Um Had plutons as well as the northwestern part of El Erediya plutons are promising zones for uranium potentiality.

These younger granites are dissected by high intensity of fractures, which create path way channels to circulate U-bearing fluids, with a seal rock like basic dykes to prevent the continuous diffusion of the U-rich fluids. The basic and lamprophyre dykes act also as heat and $CO_2$ sources required for uranium transport, (Cuney, 1997).

The trend analysis of radioelements anomalies shows that the NW-SE, NNW-SSE, NE-SW and N-S are the predominant trends. Meanwhile the WNW-ESE and NNE-SSW are the less predominant while the E-W and ENE-WSW represent the minor trends.

## FIELD INVESTIGATIONS

The field investigations are carried out to define the type of contacts of the granites with the country rocks, as well as to enable the tectonic stresses analyses of the causative tectonic events of the faults in case of fault contacts.

The field investigations are carried out on Gabal Kab Amiri through identifying and measuring the attitude of the faults contacts with the country rocks. This enabled defining the type of fault and measuring its attitude as well as the attitude of the slicken sides. Fault tectonic analysis of the collected data has been carried out to reconstruct the paleostress axes (the maximum stress; $\sigma_1$, the intermediate stress; $\sigma_2$ and the minimum stress; $\sigma_3$) through the calculation of reliable stress tensors according to Angelier (1994), (Fig. 14).

The field investigations indicate that Gabal Kab Amiri is in fault contacts with the country rocks along the NW-SE, NNE-SSW, NE-SW and E-W normal faults. The tectonic stresses analyses indicate that the area was subjected to a NE-SW extentional tectonic event, which induced neoformed NW-SE trending normal faults system, exhibiting the two conjugate normal faults sets dipping to the NE and SW directions. This event also reactivated the inherited NNE-SSW, NE-SW and E-W trending faults as normal faults creating the needed space for the emplacement of the pluton.

## CONCLUSIONS

A linear pattern was delineated in the spatial distribution of localities of well known uranium, gold and many metallic base ore deposits occurrences in the CED of Egypt.

The trends analyses and the applications of the autocorrelogram function on gravity

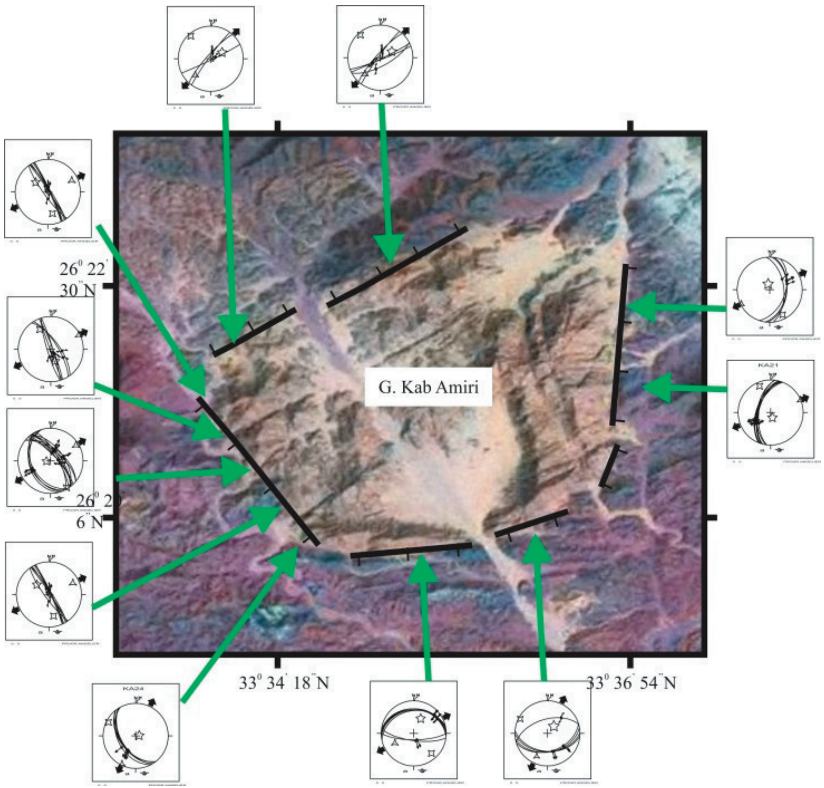


Fig. 14: Gabal (G.) Kab Amiri country rocks normal faults contacts and NE-SW extention, Central Eastern Desert, Egypt (Great circles; faults, arrows; slicken sides attitude and slip direction ☆;$\sigma_1$, ¤; $\sigma_2$, ▲; $\sigma_3$)

data indicate that the deep seated major regional fracture trends are the NW-SE, N-S, NE-SW and E-W, while they determine that the visible fracture lineaments on the Landsat image and topographic SRTM data major regional trends are the same. The trend analysis of the gamma ray spectrometric survey data indicates that the distribution of the radioelements anomalies shows that the NW-SE, NNW-SSE, NE-SW and N-S are the predominant trends. Meanwhile the WNW-ESE and NNE-SSW are the less predominant while the E-W and ENE-WSW represent the minor trends.

The field investigations indicate that Gabal Kab Amiri is in NW-SE, NE-SW and E-W faults contacts with the country rocks. Meanwhile the stress and tectonic analyses determine that the area was subjected to a NE-SW extentional tectonic event which induced neoformed NW-SE trending normal faults system, exhibiting the two conjugate normal faults sets dipping to the NE and SW directions and reactivating the inherited NNE-SSW, NE-SW and E-W trending faults as normal faults creating the needed space for the emplacement of the pluton. This determines that the granitic plutons and the spatial distribution of localities of well-known mineralization in the study area are bounded by the NW-SE, NNE-SSW, NE-SW and E-W faults due to a NE-SW extentional tectonic event.

## REFERENCES


Abdel Maguid, A.A., 1986. Geologic and radiometric studies of uraniferous granite in Um Ara-Um Shilman area, South Eastern Desert, Egypt. Ph.D. Thesis, Suez Canal Univ., Egypt, 233p.

Abdel Monem, A.A.; El-Kalioubi, B.A.; Attawiya, M.Y.; Moussa, E.M., and Ragab, A.A., 2004. Chemical characteristics and petrogenesis of pillowed arc metabasalts, Wadi Hamad, North Eastern Desert, Egypt. The 6th Inter. Conf. on Geochemistry, Alexandria Univ., Egypt.

Bakhit, F.S., 1978. Geology and radioactive mineralization of Gabal El Missikat area, Eastern Desert. Ph.D. Thesis, Ain Shams Univ., Egypt, 289p.

Dissanayake, G.; Durrant, H.; Whyte, and Bailey, T., 2000. A computationally efficient solution to the simultaneous localisation and map building (SLAM) problem. Proc. of the IEEE Int. Conf. on Robotics & Automation (ICRA), San Francisco, CA, USA, 1009-1014.

El-Balakssy, S.S., 2012. Mineralogy of the radioactive occurrence at the northern periphery of Gabal Gattar granites, North Eastern Desert, Egypt. Nuclear Sciences Scientific J., 1, 23-42.

El-Dabe, M.M., 2010. Geology, geochemistry and radioactivity of some alkali feldspar granite intrusions in the North Eastern Desert, Egypt. Ph.D. Thesis, Fac. Sci., Assiut Univ., Egypt.

El-Kassas, I.A., 1974. Radioactivity and Geology of Wadi Atalla area, Eastern Desert of Egypt. Ph.D. Thesis, Fac. Sci., Ain Shams Univ., Egypt, 502p

El-Sherif, A.M., 2005. Geology, geochemistry and radioactivity of the basement rocks, Wadi El-Ghozah area, Eastern Desert, Egypt. Ph.D. Thesis, Fac. Sci. Ain Shams Univ., Egypt, 218p.

El-Sundoly, H.I., 2008. The relation between tectonics of some granitoid rocks and radioelements distribution, Wadi Abu El-Hassan area, North Eastern Desert, Egypt. Ph.D. Thesis, Fac. Sci., South Valley Univ., Egypt.

El-Zalaky, M.A., 2007. Geology and remote sensing studies on some uranium bearing granites, Eastern Desert, Egypt. Ph.D. Thesis, Fac. Sci., Benha Univ., Egypt, 211p.

Goldschmidt, V.M., 1954. Geochemistry, The Clarendon Press, Oxford, 730p.

Hilmy, M.E., Abdel Monem, A.A., El-Kalioubi, B.A., Attawiya, M.Y. and Ragab, A.A., 2003. Polymineralization in Wadi Hammad area, North Eastern Desert, Egypt. The 5th Inter. Conf. on The Geology of the Middle East, Ain Shams Univ., Egypt, 659-683.

Khamis, H.A., 2012. Structural and radiometric studies of the Precambrian rocks at Wadi Fatira El-Zarqa area, Central Eastern Desert, Egypt. Ph.D. Thesis, Fac. Sci., Cairo Univ., Egypt.

Mahdy, N.M., 2015. A genetic model for molybdenum and uranium mineralization in Gabal Gattar granite, Northern Eastern Desert, Egypt. Ph.D. Thesis, Ain Shams Univ., Egypt, 217p.

Mason, B., 1966. The Enstatite Chondrites. Geochim Cosmochim. Acta, 30 (1), 23-26.

## تأثير العناصر التركيبية في التوزيع الفراغي لمناطق التمعدنات في محيط منطقة وادي عطا الله، وسط الصحراء الشرقية، مصر

هريدي محمد محمد هريدي

تقع منطقة وادي عطا الله بين خطي عرض ٥٩' ٢٥°و ٢٣' ٢٦° شمالاً وخطي طول ١٠' ٣٣° و ٤٠' ٣٣° شرقاً وتشمل بعضا من أكثر حالات اليورانيوم الواعدة التي ترتبط بالكتل الجرانيتية البلوتونية الحديثة مثل أم حاد وكب عميري والعرضية فضلاً عن العديد من مناجم الذهب القديمة مثل العرضية، عطاالله، الفواخير، السد وحمامه بالإضافة إلى العديد من مناجم الذهب القديمة على طول منطقة القص الكبيرة التي تمتد باتجاه شمال غرب-جنوب شرق والتي تمتد حوالي ٨٠ كم من العرضية في الشمال إلى الفواخير في الجنوب.

تظهر القياسات الحقلية المدعومة بتحليل الخطيات التركيبية لصورة القمر الصناعي لاندسات مع الخريطة الجيولوجية أن معظم هذه الخطيات لديها اتجاهات شمال غرب-جنوب شرق وشمال شرق-جنوب غرب وشمال-جنوب. تتماثل أنماط الخطيات التركيبية المستنتجة من صورة القمر الصناعي مع تلك المستنتجة من تطبيق دالة الكوريلوجرام على البيانات الطبوغرافية والجاذبية. توجد التمعدنات في الصدوع المتجهة شمال غرب-جنوب شرق والتي تتبع اصطفاف خطي يتبع الأنشطة القاعدية الماجماتية الأساسية لأخدود البحر الأحمر. يتم التحكم في التوزيع الفراغي لتمعدنات اليورانيوم والذهب من خلال الصدوع والصخور القاعدية الماجمية على الصدوع المتجهة شمال غرب-جنوب شرق. تم إعداد مجموعة من الخرائط الإشعاعية الكنتورية لمكافئات اليورانيوم والثوريوم والبوتاسيوم وتم وضع كل منهم بشكل فردي على الخريطة الجيولوجية لتحديد إمكانيات تواجد اليورانيوم. وكشفت الخرائط التي تم بناؤها أن الأجزاء الجنوبية في كل من جبل كب عميري وأم حاد وكذلك الجزء الشمالي الغربي من جبل العرضية هي مناطق واعدة لإمكانية تواجد اليورانيوم.